

Visualizing the Efficiency of a Continuously Variable Transmission

Florian Verbelen^{a,b}, Stijn Derammelaere^{a,b}, Peter Sergeant^{a,b}, Kurt Stockman^{a,b}

^a*Department of Electrical Energy, Metals, Mechanical Construction and Systems, Ghent University, Belgium*

^b*Member of Energy Efficient Drive Trains partner of Flanders Make, www.eedt.ugent.be*

Abstract

This paper investigates how the efficiency of a Continuously Variable Transmission (CVT) can be visualized in a compact way. At this point there is no standardized method to describe CVT efficiency as there are many inputs which affect the efficiency. Input speed, load torque, speed ratio and clamping force have been identified as dominant factors influencing efficiency. By analyzing the impact of each parameter a method is proposed based on an efficiency map and a scaling law. Efficiency maps are used because they represent the efficiency in the complete operating range and not only in the optimal conditions. The results of this study are of importance for constructors and end users of CVTs. The constructors benefit from the fact that they can plot the efficiency data in a compact format while the end users can use the data to optimize their drivetrain. The approach where efficiency data is used by the end users to optimize the drivetrain in terms of efficiency is called the Extended Product Approach (EPA). By implementing EPA in the design process, large savings on the long term are possible.

1. Introduction

Due to increasing fuel prices, the efficiency of drive trains and their individual components has gained a lot of interest. By optimizing the efficiency of each component in the drivetrain, large savings on the long term are possible. This is called the Extended Product Approach (EPA) and is mentioned in EN 50598.

Due to this system level optimization, knowledge of the energy efficiency over a wide range of working points of these components is vital. In contrast to the electrical parts in the drivetrain [1], [2], this information is not available for mechanical parts such as a gearbox or a Continuously Variable Transmission (CVT) which is a device with a variable speed ratio.

As with gearboxes there are many types of CVTs of which the belt CVT and the half/full toroidal CVT are the most commonly used. To limit the scope of the paper the half toroidal CVT has been chosen as subject for this study. In the half toroidal CVT, power is transmitted from the input disc to the output disc through a system of rollers (Figure 1). From the geometrical speed ratio, defined as the ratio of r_1 and r_3 , it can be seen that by varying the contact points of the rollers given by the distances r_1 and r_3 respectively, the speed ratio can be varied in a continuous way. Indeed, these contact points can be changed smoothly by manipulating the tilting angle γ of the rollers. To avoid a moving contact between two metal components and the corresponding wear, a traction fluid is used. To limit the slip in the device and thus controlling efficiency, a force called the clamping force (F_{Din}) is applied at the input disc which puts all components under a certain pressure. The main advantages of the toroidal CVT are the high torque capacity and efficiency while the main drawback is the complexity of the system.

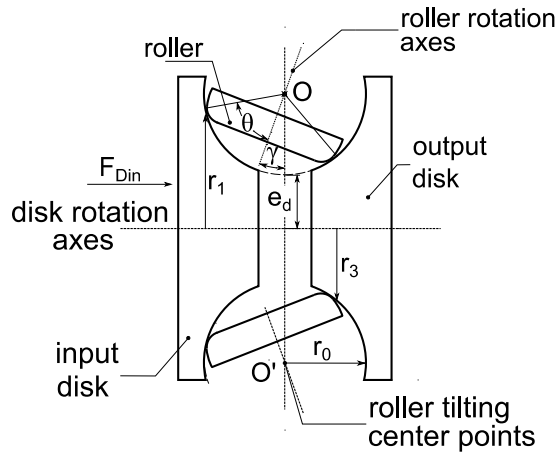


Figure 1: Schematic of a half toroidal CVT.

Some effort has already been done concerning characterization of gearboxes [3]–[5] where efficiency maps have been created displaying efficiency as function of input speed and output torque. However, for the CVT, there is not even a consensus on how to visualize the efficiency. In [6],[7] the dependency of the speed ratio and load torque on the efficiency is studied. The impact of input speed has not been considered in these studies. However, based on the measurements done in [8] some dependency on the input speed is observed.

Because there are 4 parameters (input speed, load torque, speed ratio and clamping force) which all have an impact on the efficiency, the efficiency is no longer displayable in maps. Therefore this paper presents a method to visualize efficiency data in a smart and compact format which is easy to read and understand.

This paper is structured as follows. Section 2 gives a short introduction on the model which was used to determine the efficiency values in different operating conditions. In Section 3, the boundary conditions which define the operating range of a toroidal CVT are given. Section 4 discusses the parameters which have an impact on the efficiency. In Section 5 the impact of the input speed on the efficiency is taken into account and in Section 6 an example of the proposed method is given. Finally, in Section 7 the conclusions of the research are formulated.

2. Model of the half toroidal CVT

In this paper a model of a half toroidal CVT is used to obtain the necessary efficiency data. This validated model is discussed in detail in [6] and [9] and is briefly summarized in this section.

The model consists of a contact model, a mechanical model, a simple load and a slip controller (Figure 2). In the contact model the traction conditions are determined based on the clamping force (F_{Din}), the tilting angle (γ), the input speed (ω_{in}) and output speed (ω_{out}) of the CVT. The traction conditions are used to calculate the generated torque at the input (T_{in}) and output (T_{out}).

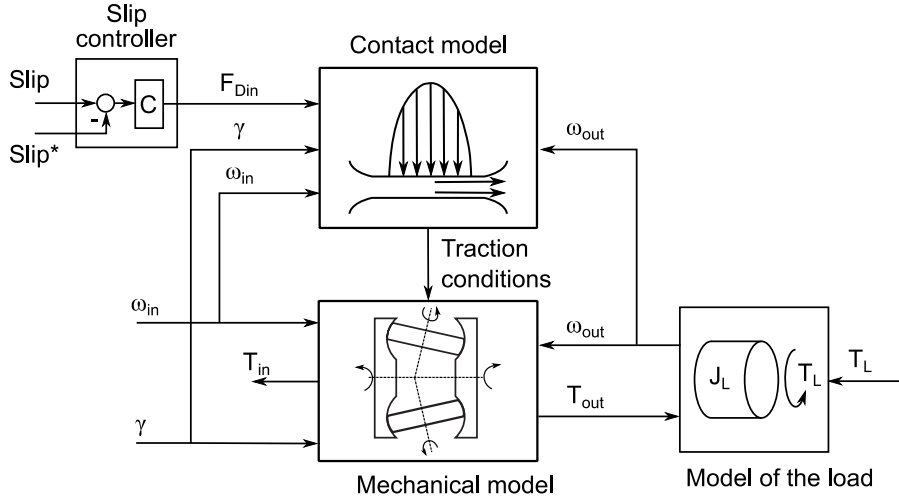


Figure 2: Model structure of the half toroidal CVT.

Slip is inevitable in a toroidal CVT and must therefore be controlled. In order to attain stable operation, slip is limited to a maximum value of 3% by the slip controller [6]. Slip can be calculated based on the following equation:

$$Slip = 1 - \frac{\tau}{S_{rID}} = 1 - \frac{\frac{\omega_{out}}{\omega_{in}}}{\frac{r_1}{r_3}} \quad (1)$$

In eq. (1), the actual speed ratio is defined as τ and the geometrical speed ratio as S_{rID} . The dynamics of the slip controller are ignored as in this paper only steady state results are considered.

3. Boundary conditions of the CVT

Boundary conditions determine the operating area of a device, in this case a CVT. A good definition of the boundary conditions is of great importance because it determines for which combination of inputs (torque, speed, speed ratio, clamping force) the efficiency should be known or not.

There are 2 types of boundary conditions: the speed ratio range and the maximum torque. The speed ratio range is defined by geometrical parameters and is limited by the input speed. Based on the geometrical parameters the maximum speed ratio S_{rIDmax} is given by:

$$S_{rIDmax} = \frac{1 + a_r}{1 + a_r - \cos\left(2\theta - \frac{\pi}{2}\right)} \quad (2)$$

Where a_r is the aspect ratio which is equal to $\frac{e_d}{r_0}$ and θ is the half cone-angle (see Figure 1). When the maximum speed ratio is known, the minimum speed ratio can easily be calculated as the inverse.

As stated in the previous paragraph the input speed can limit the maximum speed ratio. If the input speed increases, the roller speed increases. Due to the heavy loading of the rollers, special axial thrust bearings [10],[11] are used which have a rather limited maximum permissible speed. For the simulation in this paper, bearings are used with a maximum permissible speed of 6000 r/min. Figure 3a) visualizes the speed ratio limit as function of the input speed. It states that for an input speed of for example 4500 r/min the rollers will reach their limiting speed for a speed ratio of approximately 1.1.

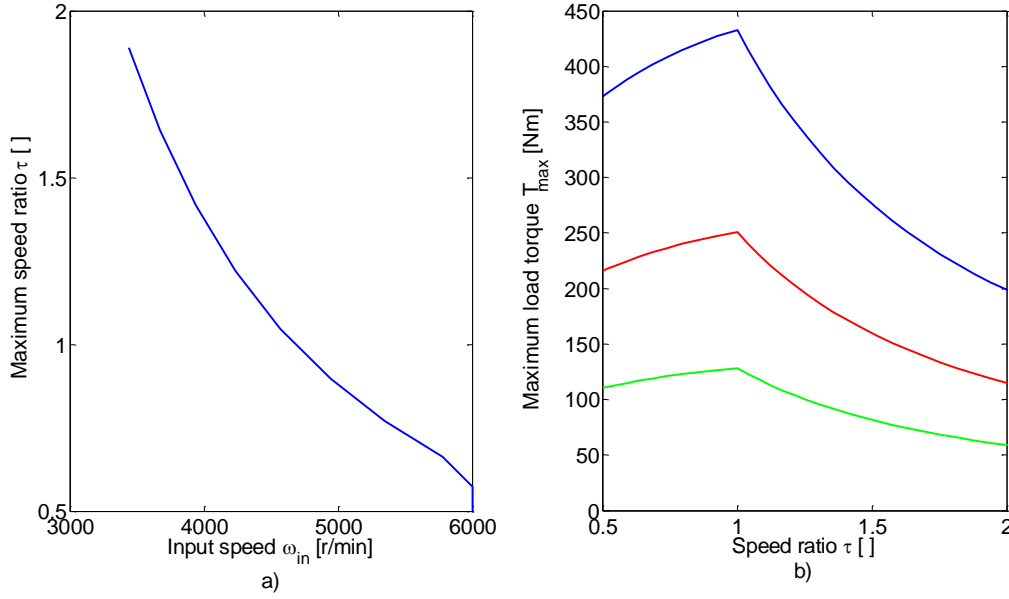


Figure 3: a) Effect of the input speed on the maximum allowable speed ratio. b) Maximum load torque as function of speed ratio for 3 maximum pressure values: 2.4 GPa (blue), 2 GPa (red) and 1.6 GPa (green).

The second boundary condition is the maximum load torque T_{max} which depends on the position of the roller γ which is related with the speed ratio τ , the maximum allowable pressure p_{max} imposed by the clamping force F_{Din} and the geometrical parameters of the CVT [9]. Figure 3b) shows that the maximum pressure plays a vital role in the torque capacity of the CVT. As the maximum pressure is defined in the design stage, the pressure will be kept constant at 2.4 GPa for the remainder of the paper. Speed has no impact on the torque capacity.

4. Efficiency of the CVT

The steady state efficiency of a CVT is calculated as follows:

$$\eta = \frac{T_L \omega_{out}}{T_{in} \omega_{in}} \quad (3)$$

This efficiency formulation can be split up in an efficiency term for speed η_ω and torque η_T :

$$\eta = \eta_\omega \eta_T \quad (4)$$

The speed efficiency term η_ω is related to the slip (see eq. (1)) while the torque efficiency η_T can be expressed in terms of traction coefficients:

$$\eta_T = \frac{\mu_{out} - \chi_{out} \sin(\theta - \gamma)}{\mu_{in} - \chi_{in} \sin(\theta + \gamma)} \quad (5)$$

In eq. (5) the input and output traction coefficients are respectively μ_{in} and μ_{out} . The spin coefficients are denoted as χ_{in} and χ_{out} . The main problem of this analytical formulation of the efficiency is that the relation with measurable parameters is lost. Therefore, the authors chose to work with eq. (3).

Based on eq. (3) it is possible to reformulate efficiency as a function F of 4 input parameters:

$$\eta = F(\omega_{in}, T_L, \tau, F_{Din}) \quad (6)$$

This 5 dimensional relation cannot be visualized in an efficiency map but the function F includes both

stable as unstable conditions. Unstable conditions are combinations of input speed, load torque, speed ratio and clamping force for which slip will increase above feasible values. It is for instance impossible to transmit torque without clamping force, independent on the input speed and speed ratio. If the unstable conditions are excluded by proper slip control through F_{Din} , eq. (6) can be rewritten as:

$$\eta_s = f(\omega_{in}, T_L, \tau) \quad (7)$$

This means that, with a proper slip controller implemented, the efficiency depends only on the input speed, the load torque and the speed ratio. This does not result in a restriction on the proposed method as a CVT is always provided to the end user with proper slip control.

The problem is now reduced from 5 to 4 dimensions. This reduction makes it possible to visualize the efficiency in an contour plot (3 dimensions) where one of the parameters is kept constant. The question remains which parameter will be kept constant and how significant the impact of that parameter is on the efficiency.

On the contour plot (Figure 4), efficiency is be plotted as function of speed ratio and load torque. This option is chosen because literature mentions torque and speed ratio as dominant parameters in terms of efficiency. Furthermore, CVTs are often used in applications where the input speed is held as constant as possible by manipulating the speed ratio as function of the load characteristics. As a consequence, input speed is kept constant but as stated in the previous paragraph, its effect on efficiency will be analyzed later on.

a) Impact of the speed ratio and load torque on the efficiency

Visualizing the efficiency in an efficiency map tells much more than a single efficiency value in optimal conditions (see Figure 4). It gives an overview on the operating range and gives an idea on how the efficiency is influenced by the operating point. The blue line on top of the operating range is the maximum torque (also shown in Figure 3b)) based on the equation presented in [9].

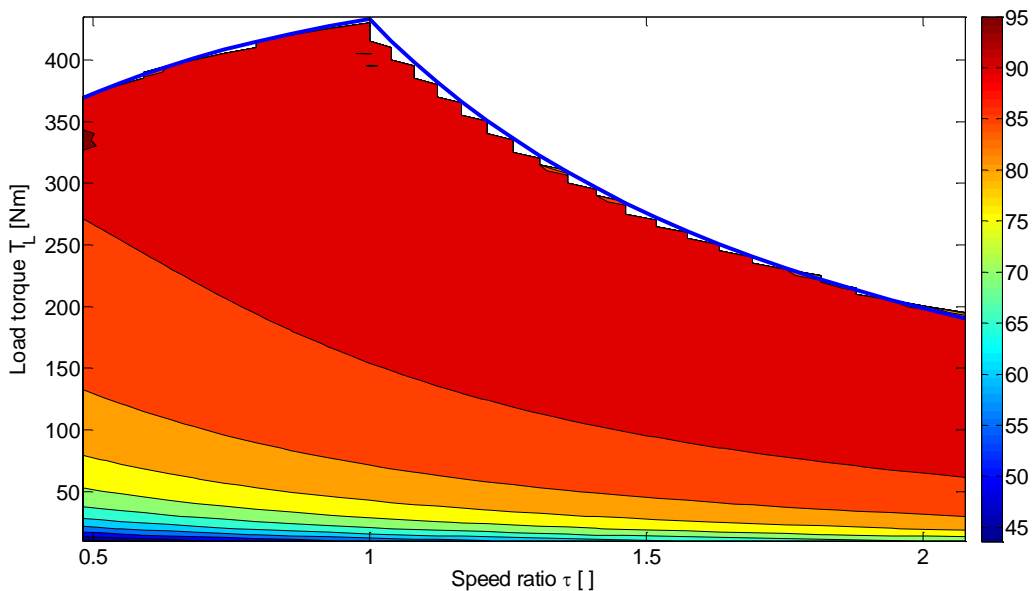


Figure 4: Efficiency of the CVT as function of speed ratio and load torque for an input speed of 3000 r/min.

b) Impact of input speed on the efficiency

The efficiency map presented in the previous subsection describes the energetic behavior at a specific input speed i.e. 3000 r/min. The question remains what the impact will be if the input speed is changed.

In Figure 5a) the input speed is varied for several different load torques and a constant speed ratio. From this figure it is possible to conclude that there is a linear trend between efficiency and input speed in the greater part of the operating range. It is also noticeable that the effect of the input speed becomes smaller for a larger load torque. In Figure 5b) the efficiency as function of varying input speed and speed ratio is shown. In terms of speed ratio it is possible to state that for a higher speed ratio, the impact of increasing input speed becomes more dominant. As with Figure 5a) there is again a linear trend noticeable. Only at low speed ratio (blue dots in Figure 5b) and low input speed there is a deviation from the linear prediction.

The bearing losses are responsible for these deviating results. The conditions for these outliers are characterized by a low bearing speed for which the losses increase rapidly for increasing input speed [12]. As the losses increase, the efficiency of the CVT decreases until an input speed of 2000 r/min. This effect diminishes at higher input speed because the bearing losses become less dominant in comparison with traction losses inside the CVT.

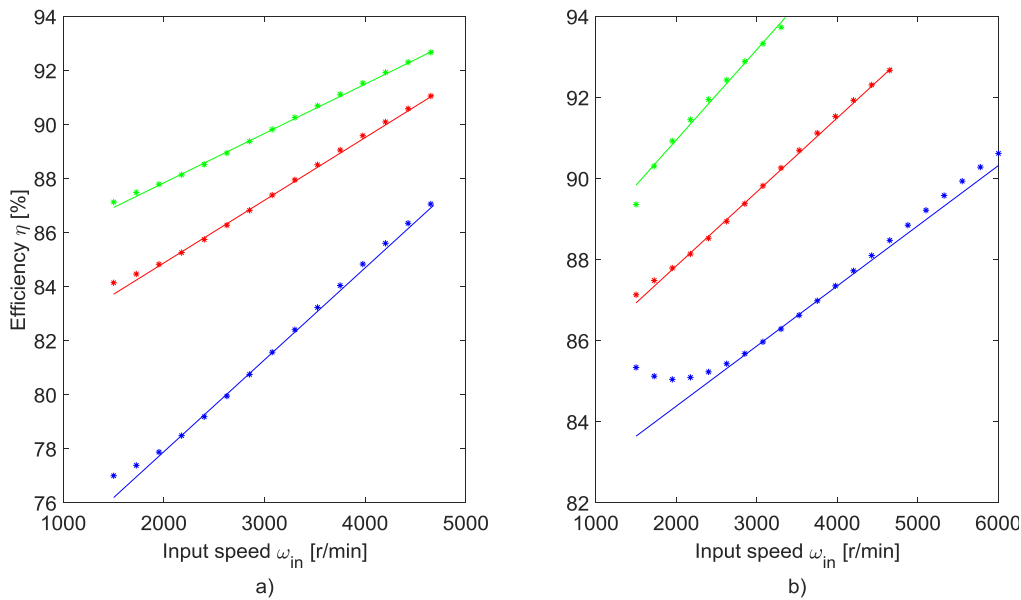


Figure 5: a) Efficiency as a function of the input speed at a speed ratio of 1 for 3 different load torques: 50Nm (blue), 100Nm (red) and 150 Nm (green). b) Efficiency as a function of the input speed at a load torque of 150Nm for 3 different speed ratio values: 0.5 (blue), 1 (red) and 2 (green).

5. Linearized efficiency

In the previous subsection a quasi linear relation was observed between input speed and efficiency. This means that the relation can be written as:

$$\eta(\tau, T_L) \approx k(\tau, T_L)\omega_{in} + c(\tau, T_L) \quad (8)$$

With k , the slope of the line, depending on speed ratio and load torque, and c the efficiency at standstill of the input shaft. As c has no physical meaning in this definition (no efficiency at standstill), eq. (8) has been rewritten as:

$$\eta(\tau, T_L) \approx k(\tau, T_L)(\omega_{in} - \omega_{ref}) + \eta_{ref}(\tau, T_L) \quad (6)$$

With ω_{ref} a certain reference speed in rad/s and η_{ref} the efficiency at the chosen reference speed for a given speed ratio and load torque. This expression describes the relation between an efficiency map $\eta_{ref}(\tau, T_L)$ defined at a certain reference speed ω_{ref} and an efficiency map $\eta(\tau, T_L)$ at a different input speed ω_{in} via the factor $k(\tau, T_L)$. In other words: the reference efficiency map becomes scalable via $k(\tau, T_L)$. The only question which remains is how $k(\tau, T_L)$ has to be defined.

Because it is not feasible to determine k for all possible speed ratio and load torque combinations a selection of points is proposed where k will be determined. These points are chosen based on speed ratio values which are spread throughout the speed ratio range and corresponding torque values which are equal to 95%, 50% and 25% of the maximum load torque (Figure 6). Another feature which has been added to Figure 6 are red lines indicating the maximum speed ratio for a given input speed. These lines are a projection of Figure 3a on the operating range and indicate clearly how the input speed will limit the operating range.

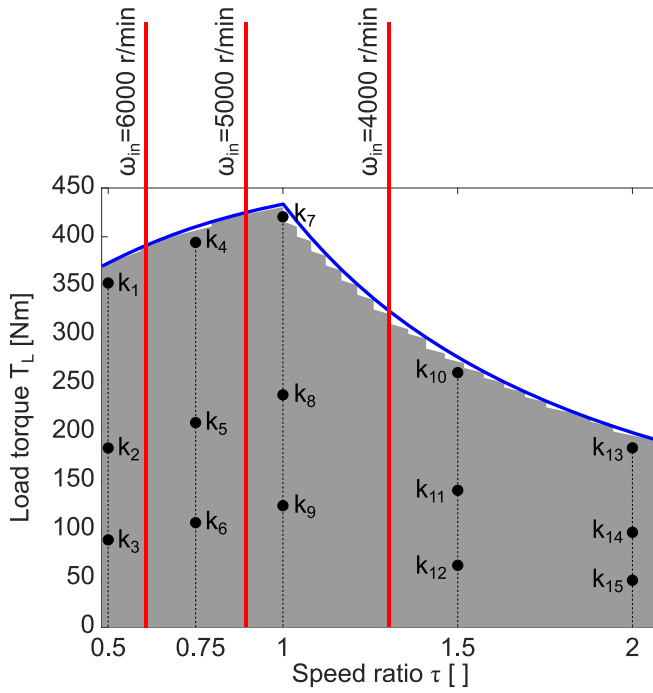


Figure 6: Location of the k values and boundary condition for torque (blue line) and speed ratio (red lines).

The results for the k values are given below:

$$K = \begin{bmatrix} k_1 & k_4 & k_7 & k_{10} & k_{13} \\ k_2 & k_5 & k_8 & k_{11} & k_{14} \\ k_3 & k_6 & k_9 & k_{12} & k_{15} \end{bmatrix} = 10^{-6} \times \begin{bmatrix} 83.82 & 91.75 & 94.72 & 148.15 & 188.85 \\ 124.41 & 142.45 & 140.55 & 208.43 & 266.12 \\ 187.04 & 204.07 & 211.62 & 307.04 & 391.52 \end{bmatrix} \quad (7)$$

The corresponding efficiencies can be found in the efficiency map (Figure 4) but are given here for the convenience.

$$\eta_{ref} = \begin{bmatrix} \eta_1 & \eta_4 & \eta_7 & \eta_{10} & \eta_{13} \\ \eta_2 & \eta_5 & \eta_8 & \eta_{11} & \eta_{14} \\ \eta_3 & \eta_6 & \eta_9 & \eta_{12} & \eta_{15} \end{bmatrix} = 10^{-2} \times \begin{bmatrix} 90.93 & 92.26 & 92.96 & 93.6 & 93.87 \\ 87.42 & 89.86 & 91.35 & 91.51 & 91.67 \\ 81.61 & 85.36 & 87.74 & 87.79 & 88.02 \end{bmatrix} \quad (8)$$

6. Numerical example

Figure 7 gives an overview of a numerical example at an input speed of 2000 r/min and 4000 r/min. The reference input speed is 3000 r/min. In Figure 7 simulation results (a) and (b) are compared with calculated results (c) and (d). To demonstrate the ease of the procedure, the highlighted number in Figure 7 c) is elaborated in the next paragraph.

The input speed is 4000 r/min and the reference speed is 3000 r/min. The marked location on Figure 7 c) is known as location 8 in Figure 6 which means k_8 and η_8 are needed. When these numbers are filled out in eq. (9), this results in:

$$\eta(\tau, T_L) \approx 140.55 \times 10^{-6} \left(\frac{4000.2\pi}{60} - \frac{3000.2\pi}{60} \right) + 91.35 \times 10^{-2} = 0.928 \quad (9)$$

The actual efficiency for that operating point, as simulated, is 93,1% which means that the efficiency is estimated with an error of 0.3%. If all considered points are taken into account, it is possible to state that the efficiency can be estimated with a mean error of 0.33% and a maximum error of 1%. This proves that a combination of Figure 4 and 6 could be very useful for end users of CVTs as it enables them to calculate the efficiency of every possible operating point within reasonable error bands.

If the end users are interested in a point for which there is no predefined k value, for example for a speed ratio of 0.9 and a load torque of 150Nm, it is possible to calculate the efficiency by interpolation between the surrounding efficiencies (location 5, 6, 8 and 9).

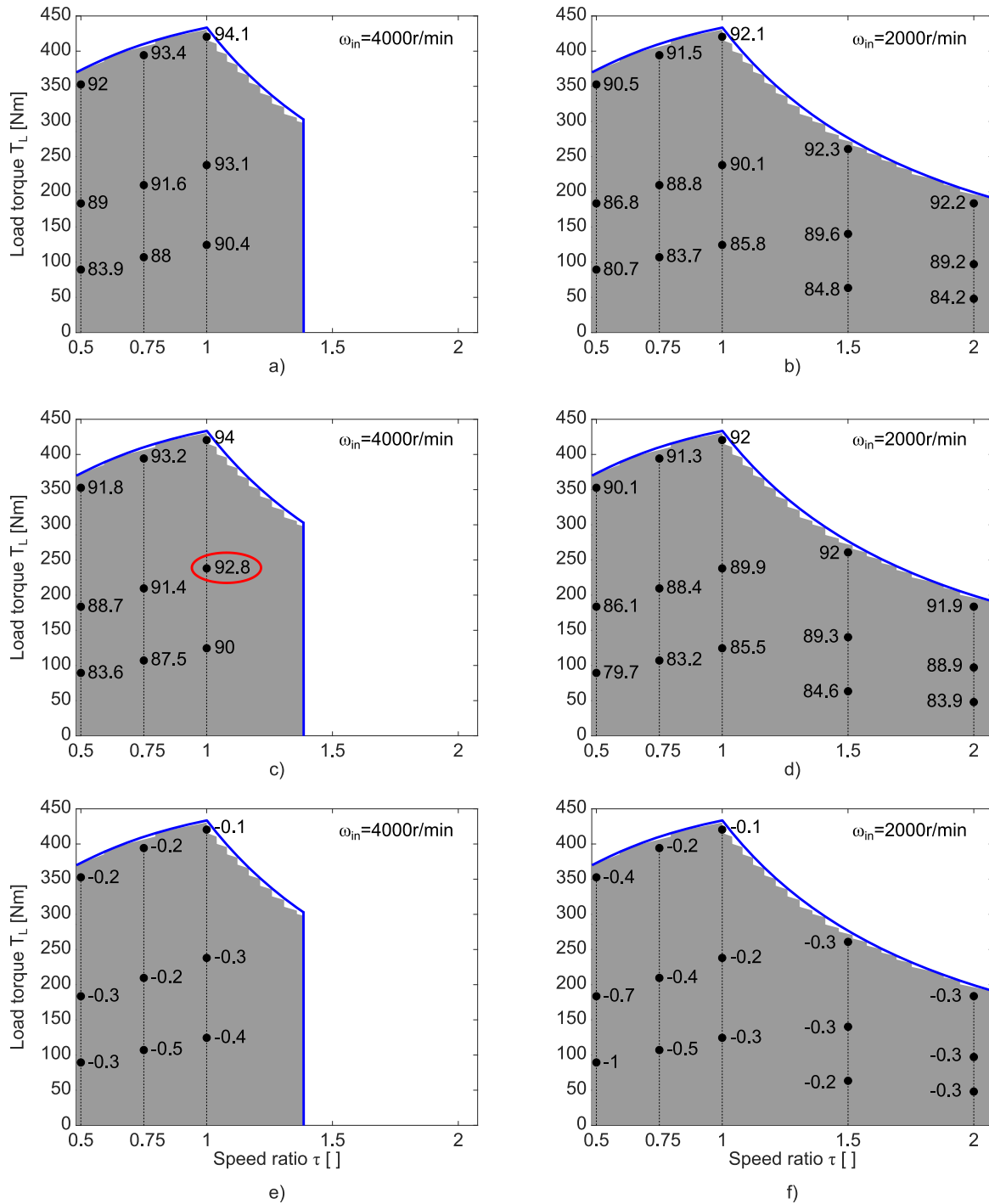


Figure 7: a) - b) Simulated efficiency values [%]. c) - d) Calculated efficiency values [%] based on eq. (9). e) - f) Error [%] on the presented method.

7. Conclusion

This paper discusses how the efficiency of a Continuously Variable Transmission can be visualized in a compact format. Efficiency can be written as function of input speed, load torque, speed ratio and clamping force which makes it unpractical to visualize efficiency in contour plots. The impact of clamping force can be eliminated if a proper slip controller is considered. By defining efficiency as a function of speed ratio and load torque it is possible to visualize the efficiency on a contour plot but then the impact of the input speed is neglected. In this paper it is shown that there is a linear relation

between the efficiency and the input speed. By characterizing this linear relation, an equation could be set up which makes it possible to rescale a given efficiency map at a certain input speed to an efficiency map defined at a different input speed. A numerical example is added and it is shown that the mean error of the method is limited to 0.33%.

8. Acknowledgement

This research is carried out for the EMTechno project (project ID: IWT150513) supported by VLAIO and Flanders Make, the strategic research center for the manufacturing industry.

9. References

- [1] K. Stockman, S. Dereyne, D. Vanhooydonck, W. Symens, J. Lemmens, and W. Deprez, "Iso efficiency contour measurement results for variable speed drives," in *19th International Conference on Electrical Machines, ICEM 2010*, 2010.
- [2] "Manufacturer's statement on Abb.com, (2017). ABB IE4 SynRM Motor-Drive Packages - Synchronous Reluctance Motor-Drive Packages.," Accessed 26 June 2017. [Online]. Available: <http://www.abb.com/product/seitp322/51c4b5bba1fa1372c125785d003d389b.aspx> .
- [3] S. Dereyne, E. Algoet, P. Defreyne, and K. Stockman, "An energy efficiency measurement test bench for gearboxes," in *Energy efficiency of Motor Driven Systems*, 2013.
- [4] S. Derammelaere, S. Dereyne, P. Defreyne, E. Algoet, F. Verbelen, and K. Stockman, "Energy efficiency measurement procedure for gearboxes in their entire operating range," *Ind. Appl. Soc. Annu. Meet. 2014 IEEE*, pp. 1–9, 2014.
- [5] S. Dereyne, P. Defreyne, E. Algoet, and S. Derammelaere, "Efficiency measurement campaign on gearboxes," in *Energy efficiency of Motor Driven Systems*, 2015, pp. 1–11.
- [6] G. Carbone, L. Mangialardi, and G. Mantriota, "A comparison of the performances of full and half toroidal traction drives," *Mech. Mach. Theory*, vol. 39, no. 9, pp. 921–942, 2004.
- [7] H. Tanaka, N. Toyoda, H. Machida, and T. Imanishi, "Development of a 6 Power-Roller Half-Toroidal CVT," *NSK Tech. J. Motion Control*, vol. 9, pp. 15–26, 2000.
- [8] T. Yamamoto, "Analysis of the efficiency of a half-toroidal CVT," *JSAE Rev.*, vol. 22, no. 4, pp. 565–570, 2001.
- [9] F. Verbelen, S. Derammelaere, P. Sergeant, and K. Stockman, "Half toroidal continuously variable transmission: trade-off between dynamics of ratio variation and efficiency," *Mech. Mach. Theory*, vol. 107, pp. 183–196, 2017.
- [10] T. Imanishi and S. Miyata, "Development of the Next-Generation Half-Toroidal CVT," *Motion Control*, vol. 14, no. 5, pp. 20–24, 2003.
- [11] R. Fuchs, N. Mccullough, and K. Matsumoto, "The Making of the Full Toroidal Variator," *JTEKT Eng. J.*, no. 1006E, pp. 31–36, 2009.
- [12] SKF, "Rolling bearing catalogue," 2013.